Exciton Delocalization in the B808–866 Antenna of the Green Bacterium *Chloroflexus aurantiacus* as Revealed by Ultrafast Pump-Probe Spectroscopy

Vladimir Novoderezhkin and Zoya Fetisova
A. N. Belozersky Institute of Physico-Chemical Biology, Moscow State University, Moscow 119899, Russia

ABSTRACT A model of pigment organization in the B808–866 bacteriochlorophyll *a* antenna of the green photosynthetic bacterium *Chloroflexus aurantiacus* based on femtosecond pump-probe studies is proposed. The building block of the antenna was assumed to be structurally similar to that of the B800–850 light-harvesting 2 (LH2) antenna of purple bacteria and to have the form of two concentric rings of *N* strongly coupled BChl866 pigments and of *N*/2 weakly coupled BChl808 monomers, where $N = 24$ or 32. We have shown that the Q_y transition dipoles of BChl808 and BChl866 molecules form the angles $43° \pm 3°$ and $8° \pm 4°$, respectively, with the plane of the corresponding rings. Using the exciton model, we have obtained a quantitative fit of the pump-probe spectra of the B866 and B808 bands. The anomalously high bleaching value of the B866 band with respect to the B808 monomeric band provided the direct evidence for a high degree of exciton delocalization in the BChl866 ring antenna. The coherence length of the steady-state exciton wave packet corresponds to five or six BChl866 molecules at room temperature.

INTRODUCTION

The initial steps of photosynthesis comprise the absorption of light and excitation energy transfer in a light-harvesting antenna with a subsequent excitation trapping by a reaction center in which charge separation is started (van Grondelle et al., 1994). In purple photosynthetic bacteria the light-harvesting antenna consists of a peripheral antenna (LH2) and a core antenna (LH1) that directly surround the reaction centers. The energy transfer among pigment molecules in the antenna has been described by incoherent hopping theory (Pullerits et al., 1994; Somsen et al., 1994; Visser et al., 1995). An exciton model of energy transfer in the antenna assuming exciton delocalization over a large number of pigment molecules was proposed as well (Novoderezhkin and Razjivin, 1993, 1994, 1995a; Dracheva et al., 1995).

The first high-resolution three-dimensional x-ray structure was obtained for the peripheral LH2 antenna of purple bacteria *Rhodopseudomonas acidophila* (McDermott et al., 1995) and *Rhodospirillum molischianum* (Koepke et al., 1996). It was shown that these antenna complexes consist of α-β pigment-protein subunits arranged in a high-symmetry ring-like structure. For example, the LH2 antenna of *R. acidophila* contains 9 α-β subunits, each binding two bacteriochlorophyll 850 (BChl850) molecules and one BChl800 molecule. Moreover, it was shown that 18 BChl850 molecules form the C_9-symmetry ring with a dimeric unit cell, whereas nine BChl800 molecules form the C_9-symmetry ring with a monomeric unit cell in a parallel plane. The Mg-Mg distance between BChl850 pigments bound to the same α,β-polypeptide unit is 0.87 nm, and the distance between nearest BChl850 pigments of neighboring dimeric units is 0.97 nm. The distances between nearest BChl800 molecules and between nearest BChl800 and BChl850 molecules are larger (2.1 nm and 1.8 nm, respectively). The structure of the LH2 antenna of *R. molischianum* is similar to that of *R. acidophila*, but this antenna complex consists of eight α-β pigment-protein subunits.

These reports have stimulated renewed interest in the electronic structure of these antennae (Dracheva et al., 1996, 1997; Jimenez et al., 1996; Alden et al., 1997; Hu et al., 1997; Koolhaas et al., 1997; Monshouwer et al., 1997). Different estimations of the interaction energies and the site inhomogeneity value in these papers result in different evaluations of the degree of exciton delocalization in the antenna.

The direct estimation of the exciton delocalization degree can be obtained by using difference absorption spectra (Novoderezhkin and Razjivin, 1993). For the B800–850 antenna one can compare the bleaching value of the B850 band and that of the B800 monomeric band (Kennis et al., 1996). In the case of the core LH1 antenna one can compare the bleaching amplitudes of the antenna and of the BChl dimer of the reaction center (Novoderezhkin and Razjivin, 1993, 1995b; Kennis et al., 1994; Xiao et al., 1994). Analysis of experimental data has shown an anomalously high dipole strength of the bleached transitions reflecting highly delocalized exciton states within the LH2 and LH1 antennae (Novoderezhkin and Razjivin, 1993, 1995b; Kennis et al., 1994; Xiao et al., 1994; Leupold et al., 1996). The exciton delocalization degree can also be estimated by using the shape of difference absorption spectra (van Burgel et al., 1995; Pullerits et al., 1996; Chachisvilis et al., 1997; Meier et al., 1997; Kühn and Sundström, 1997).

Received for publication 6 November 1998 and in final form 8 March 1999.

Address reprint requests to Dr. Zoya G. Fetisova, A. N. Belozersky Institute of Physico-Chemical Biology, Moscow State University, Bldg. A, 119899 Moscow, Russia. Tel.: 07-095-939-53-63; Fax: 07-095-9393181; E-mail: fzg@pa.genebee.msu.su.

0006-3495/99/07/424/07 $2.00

In this paper we analyze the shape and amplitude of difference absorption spectra of the membrane-bound B808–866 BChl *a* antenna of the green thermophilic bacterium *Chloroflexus aurantiacus* (Novoderezhkin et al., 1998). There are experimental data allowing one to assume that the B808–866 antenna is made up of structural units similar to that of the B800–850 LH2 antenna of purple bacteria. The B808–866 and B800–850 LH2 antennas exhibit parallels in their protein structure, absorption spectra, and energy transfer kinetics. The B808–866 complex contains α- and β-polypeptides in a 1:1 ratio. The α- and β-proteins show three-domain structures reminiscent of LH2. They exhibit 27–30% sequence homologies to the LH2 α- and β-polypeptides (Wechsler et al., 1985, 1987; Zuber and Brunisholz, 1991). Furthermore, each B808–866 polypeptide has a histidine residue within its hydrophobic α-helical domain that could coordinate a BChl *a* pigment. These B808–866 complexes surround the P870 reaction centers in the cytoplasmic membrane; in this respect, they resemble LH1 complexes of purple bacteria.

Recently, the room temperature excited-state kinetics of the membrane-bound B808–866 antenna of *C. aurantiacus* were reported (Novoderezhkin et al., 1998). Two-color isotropic and anisotropic kinetics of B808→866 energy transfer were measured under femtosecond resolution. This allowed one to measure the shapes and amplitudes of absorbance difference spectra of the B808 and B866 bands of this antenna.

We propose here a model of the B808–866 antenna that allows us to explain all of the features of pump-probe spectra obtained in the femtosecond pump-probe experiment (Novoderezhkin et al., 1998) and to estimate the effective exciton size in the antenna.

MODEL OF THE B808–866 ANTENNA

We suppose that the structure of the B808–866 antenna is analogous to that of the B800–850 LH2 antenna of purple bacteria. As a model of an antenna unit, we consider two concentric circular aggregates that lie in two planes parallel to the membrane plane. The first one consists of N strongly coupled BChl866 molecules and has $C_{N/2}$ symmetry with a dimeric unit cell. The second ring consists of $N/2$ BChl808 weakly coupled molecules and has $C_{N/2}$ symmetry with a monomeric unit cell. We assume that the N value for the B808–866 antenna is the same as for the LH1 core antenna of purple bacteria, i.e., $N = 24$ or 32 (Karrasch et al., 1995). The Q_y transition dipole moments of two BChl866 molecules in a dimeric unit cell form angles ψ_1 and ψ_2 with the circle plane, and angles φ_1 and φ_2 with the tangent to the circle. The electronic transition energy of BChl866 pigments is E. The corresponding parameters for BChl808 pigments are ψ', φ', and E'. In our simulations we have taken into account the interactions between the Q_y transitions of BChls, neglecting their mixing with the Q_x, B_y, and B_x transitions as well as with charge transfer states (Alden et al., 1997).

We suppose that the interaction energies between BChl866 molecules are $M_{12} = 400\ cm^{-1}$, $M_{23} = 290\ cm^{-1}$, $M_{13} = -52\ cm^{-1}$, and $M_{14} = 14\ cm^{-1}$, where M_{12} corresponds to the intradimer interactions, M_{23} to the interdimer nearest-neighboring interactions, M_{13} to the second-neighbor interactions, and M_{14} to the third-neighbor interactions. These values correspond to the best fit of experimental spectra (see below). Note that microscopic calculations using the point charge approximation give $M_{12} = 806\ cm^{-1}$, $M_{23} = 377\ cm^{-1}$, $M_{13} = -152\ cm^{-1}$ for the LH2 complex of *R. molischianum* (Hu et al., 1997), and $M_{12} = 197$–$545\ cm^{-1}$, $M_{23} = 158$–$461\ cm^{-1}$, with the various treatments of the dielectric screening for the LH2 complex of *R. acidophila* (Alden et al., 1997). We also supposed that the interaction energy between BChl808 pigments is on the same order of magnitude as the interaction energy between BChl800 pigments in the LH2 antenna, i.e., $\sim$15–30 cm^{-1} (Alden et al., 1997). So excitonic interactions determine the greater part of the actual red shift of B866 and B808 bands. To obtain the true positions of 808-nm and 867-nm peaks, we introduced some additional red shifts to E' and E (i.e., two different ones).

The site inhomogeneity of the antenna was described by noncorrelated perturbations $\delta E'$ and δE to electronic energies of BChl808 and BChl866 pigments, E' and E. We assumed that $\delta E'$ and δE have a Gaussian distribution. The width (FWHM) of this distribution, σ (the same for $\delta E'$ and δE), was varied from 0 to 1000 cm^{-1}. Notice that spectral disorder in a real antenna of $\sim$300–600 cm^{-1} will completely destroy the exciton delocalization within the B808 ring (which is similar to the finding for LH2 antenna; Dracheva et al., 1997). For this reason we supposed the monomeric nature of the B808 band. The validity of this assumption was confirmed by our pump-probe experiments (Novoderezhkin et al., 1998).

To calculate absorbance difference spectra of the B866 band, we used the method of direct numerical diagonalization of one- and two-exciton Hamiltonian and Monte Carlo averaging over a random distribution of diagonal energies modeling the site inhomogeneity. We used the standard Hamiltonian for a Frenkel exciton in the Heitler-London approximation for two-level molecules (Davydov, 1971; Agranovich and Galanin, 1982). The exciton-phonon interactions were not taken into account. To calculate the homogeneously broadened spectra (for each set of diagonal energies), we assumed the Gaussian lineshape with homogeneous linewidths (FWHM) Γ_{1L}, Γ_{1H}, Γ_{2L}, Γ_{2H}, corresponding to the transitions from the ground state to the lowest one-exciton level (Γ_{1L}), from the ground state to higher one-exciton levels (Γ_{1H}), from the lowest one-exciton level to two-exciton levels (Γ_{2L}), and from higher one-exciton levels to two-exciton levels (Γ_{2H}). The Stokes shift of stimulated emisson of one-exciton levels is S. Parameters Γ_{1L}, Γ_{1H}, Γ_{2L}, Γ_{2H}, and S should be determined from fitting of experimental data.

The shape of difference absorption of the B866 band is determined by photobleaching (PB) and stimulated emis-

sion (SE) of one-exciton levels and by excited-state absorption (ESA) due to transitions from one-exciton states to two-exciton states. The most intensive ESA lines are blue shifted with respect to the PB/SE lines, giving rise to a specific sigmoid spectrum that is typical of a circular aggregate (Novoderezhkin and Razjivin, 1993). The very important manifestation of exciton delocalization is an increase in amplitudes of the PB, SE, and ESA components proportional to the dipole strength of exciton transitions (Novoderezhkin and Razjivin, 1993, 1995a). The dipole strength of the most intensive transitions is determined by N_{eff}, where N_{eff} is an effective delocalization length of individual exciton states (Dracheva et al., 1997). But the ΔA value is not just simply proportional to N_{eff}, being determined also by an overlap of spectral lines of different excition transitions within the PB, SE, and ESA spectra, as well as by an overlap of the negative PB/SE and positive ESA components (Mukamel, 1995; Dracheva et al., 1997).

The difference spectrum of the BChl808 monomer is determined by single PB and SE lines (we neglect the ESA due to higher singlet levels). The width of these lines is Γ_{M}; the monomeric Stokes shift is S_{M}.

RESULTS

Shape and amplitude of difference absorption

Calculated and measured pump-probe spectra are shown in Fig. 1 for zero time delay (immediately after excitation of the B808 band) and for 8-ps delay corresponding to complete B808→B866 energy transfer (the B808→B866 energy transfer occurs with a time constant of 1.5–2 ps; Novoderezhkin et al., 1998). Experimental data show that the ratio of bleaching amplitudes of the B808 and B866 bands (absorbance changes at 811 and 882 nm) is 2.72. When excluding the coherent spike (which has ~17% of the total amplitude of the signal at 811 nm), this ratio is equal to 3.29. It is difficult to obtain the true ratio of integrated intensities of the bleaching peaks because the maximum probe wavelength in our experiments, 900 nm, corresponds to the middle of the red end of the difference spectrum. When the B866 bleaching peak is integrated from 863 nm to 900 nm, the ratio approaches 5. This value should be considered as a lower limit. The best fit of the experimental spectra was obtained for $N = 24$, $\Gamma_{1L} = 270\ \mathrm{cm}^{-1}$, $\Gamma_{1H} = 400\ \mathrm{cm}^{-1}$, $\Gamma_{2L} = 420\ \mathrm{cm}^{-1}$, $\Gamma_{2H} = 445\ \mathrm{cm}^{-1}$, $\Gamma_{M} = 240\ \mathrm{cm}^{-1}$, $S = 120\ \mathrm{cm}^{-1}$, $S_{M} = 110\ \mathrm{cm}^{-1}$, and $\sigma = 410\ \mathrm{cm}^{-1}$ (Fig. 1). The N value was fixed (i.e., $N = 24$ or 32); all other parameters were determined from the fit with an accuracy of about ±5%.

To study the relation between the size of the aggregate and its nonlinear response, we have calculated pump-probe spectra for $N = 18$, 24, and 32 (Fig. 2). All parameters are the same as in Fig. 1. When N increases, the bleaching amplitude (i.e., the amplitude of the PB/SE peak) increases, but not in proportion to N, because of an overlap of the ESA and PB/SE components.

The spectra calculated for $N = 24$ and $\sigma = 0$, 410, and 700 cm^{-1} are shown in Fig. 3. The spectral features of the difference absorption, such as the shape, the amplitude, and the red shift, are shown to be strongly dependent on the site inhomogeneity value.

We also performed the calculations with alternative choices for the interaction energies: $M_{12} = 260$ and 600 cm^{-1} instead of $M_{12} = 400\ \mathrm{cm}^{-1}$ (Fig. 4). For both of the

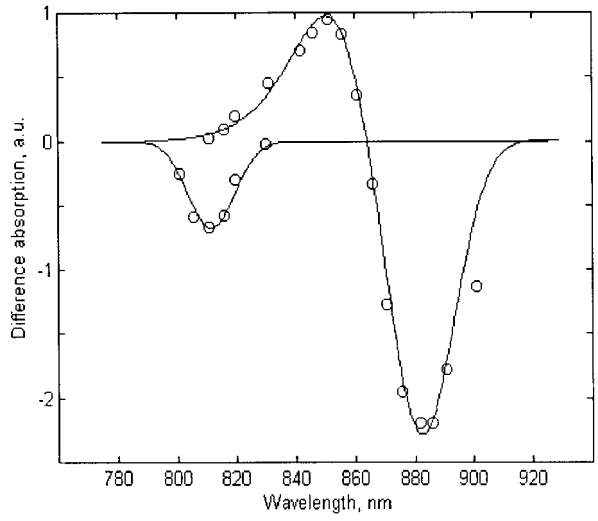

FIGURE 1 Experimental pump-probe spectra for the B808–866 antenna of *Chloroflexus aurantiacus* at 0 and 8-ps delay after 808-nm excitation (○) and calculated spectra (——). Parameters of the B866 band: $N = 24$; interaction energies are $M_{12} = 400\ \mathrm{cm}^{-1}$, $M_{23} = 290\ \mathrm{cm}^{-1}$, $M_{13} = -52\ \mathrm{cm}^{-1}$, and $M_{14} = 14\ \mathrm{cm}^{-1}$; the linewidths are $\Gamma_{1L} = 270\ \mathrm{cm}^{-1}$, $\Gamma_{1H} = 400\ \mathrm{cm}^{-1}$, $\Gamma_{2L} = 420\ \mathrm{cm}^{-1}$, $\Gamma_{2H} = 445\ \mathrm{cm}^{-1}$; the Stokes shift is $S = 120\ \mathrm{cm}^{-1}$; the site inhomogeneity is $\sigma = 410\ \mathrm{cm}^{-1}$. The linewidth and Stokes shift for the monomeric B808 band are $\Gamma_{M} = 240\ \mathrm{cm}^{-1}$ and $S_{M} = 110\ \mathrm{cm}^{-1}$, respectively.

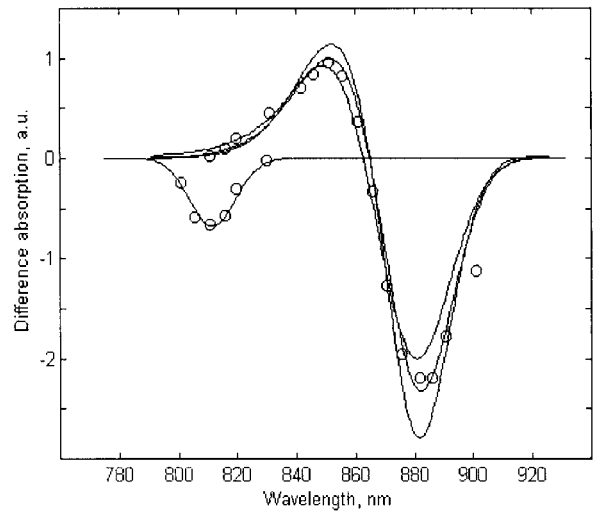

FIGURE 2 The same spectra as in Fig. 1, but calculated curves correspond to three different antenna sizes, N. In increasing order of the bleaching amplitude of the B866 band, the antenna sizes are $N = 18$, 24, and 32. All other parameters are the same as in Fig. 1. The spectrum for the monomeric B808 band does not depend on N.

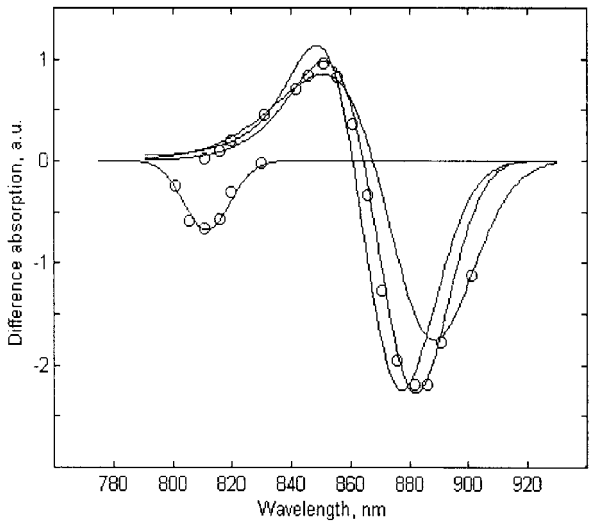

FIGURE 3 The same spectra as in Fig. 1, but calculated curves correspond to three different values of the site inhomogeneity of the BChl866 antenna, i.e., $\sigma = 0$, 410, and 700 cm^{-1}. The increase in σ corresponds to the increasing red shift of the bleaching peak of the B866 band. All other parameters are the same as in Fig. 1.

alterations of M_{12} we performed a corresponding scaling of M_{23}, M_{13}, and M_{14}.

From Figs. 2–4 one can see that the bleaching amplitude increases when the aggregate size and the interaction energy value increase, but decreases with an increase in the site inhomogeneity. This is not surprising, because the delocalization length, N_{eff}, should be proportional to N and inversely proportional to the σ/M_{12} ratio, which is responsible for destruction of delocalized excition states (Dracheva et al., 1997). It means that we may reproduce the experimental

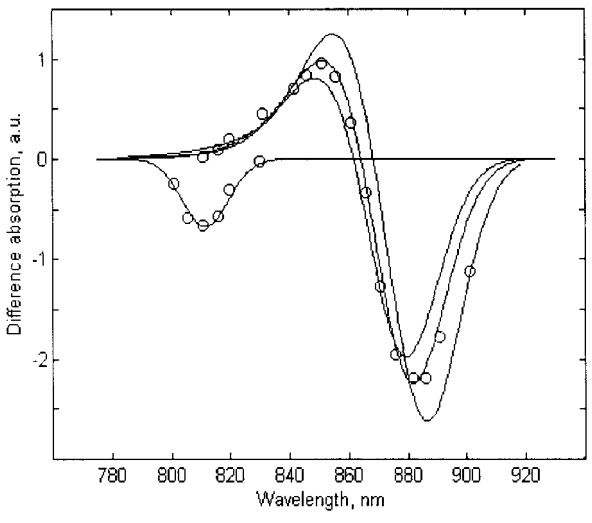

FIGURE 4 The same spectra as in Fig. 1, but calculated curves correspond to three different sets of interaction energies. In increasing order of the bleaching amplitude of the B866 band, the largest interaction energy, M_{12}, is 260, 400, and 600 cm^{-1}. For these values of M_{12} we performed a corresponding scaling of M_{23}, M_{13}, and M_{14}. All other parameters are the same as in Fig. 1.

bleaching amplitude by using simultaneous variations in N and σ (when M_{12} = constant) or by variations in M_{12} and σ (when N = constant). For example, a reasonable fit of the shape and the amplitude of difference absorption may be obtained for $N = 32$ and $\sigma = 600$ cm^{-1} instead of $N = 24$ and $\sigma = 410$ cm^{-1} (when $M_{12} = 400$ cm^{-1}). We have also obtained a satisfactory fit for $\sigma = 290$ or 560 cm^{-1}, when $M_{12} = 260$ or 600 cm^{-1}, respectively ($N = 24$). However, these alternative fits are not as good as the fit in Fig. 1 (data not shown). Parameters of different fits under investigation are listed in Table 1.

Induced absorption anisotropy

The steady-state (residual) pump-probe anisotropy in the B866 band excited at 882 nm is close to 0.1 (Novoderezhkin et al., 1998). This value corresponds to the in-plane orientation of Q_y transition dipoles of BChl866. Some deviation from 0.1 is a result of the nonzero angle between the dipole moment and the circle plane. Comparison of measured and calculated anisotropy values shows that the ψ_1 and ψ_2 values do not exceed $8° \pm 4°$ (data not shown).

The residual anisotropy in the B866 band excited at 808 nm is negative, varying from -0.03 to -0.05. These data allowed us to determine the orientation of the Q_y transition dipoles of BChl808. The angle between the BChl808 Q_y transition dipole and the circle plane was found to be $\psi' = 43° \pm 3°$. A similar result was obtained by Vasmel et al. (1986).

Exciton delocalization

Quantitative information about the delocalization of the exciton wave functions can be obtained using the so-called participation ratio L (Fidder et al., 1991), which is equal to $(N_{eff})^{-1}$, where N_{eff} is an effective delocalization length of the wave function, corresponding to an individual exciton state, averaged over disorder. The participation ratios calculated for the B866 antenna for $N = 24$ and $N = 32$ are shown in Fig. 5. The width of exciton levels in this calculation was taken to be 3 cm^{-1}; all other parameters were taken from fits 2 and 4 (see Table 1). For both of these cases we have obtained $L = 0.08–0.1$ near the absorption maximum (850–870 nm). It means that the individual exciton states in the B866 antenna are delocalized over 10–12 BChl866 molecules. The similar result was obtained for the

TABLE 1 Optimized parameters for the fits of absorption difference spectra of the B808-866 antenna of *Chloroflexus aurantiacus*

Fit	N	M_{12} (cm^{-1})	σ (cm^{-1})	Comments
1	24	260	290	Data not shown
2	24	400	410	See Fig. 1
3	24	600	560	Data not shown
4	32	400	600	Data not shown

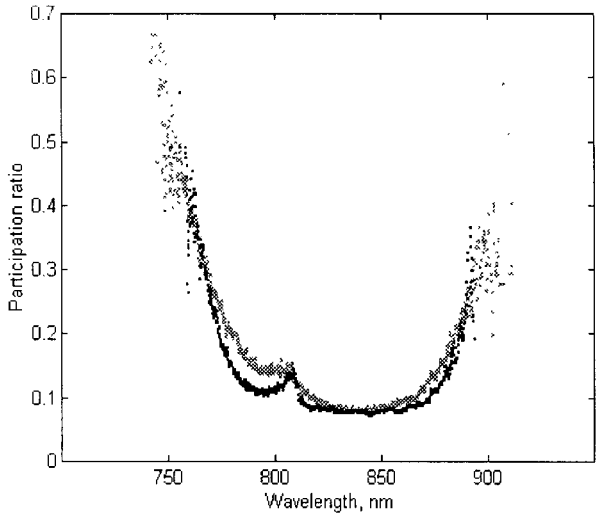

FIGURE 5 The participation ratio calculated for the BChl866 antenna for $N = 24$ (*lower curve*) and $N = 32$ (*upper curve*). The width of exciton levels was taken to be 3 cm^{-1}; all other parameters were taken from fits 2 and 4 (see Table 1).

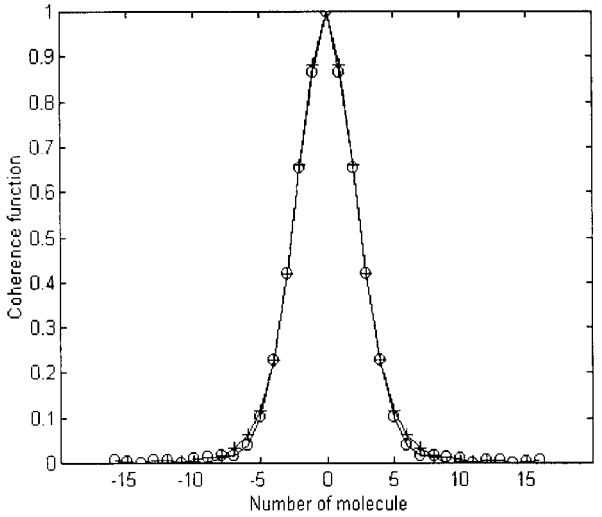

FIGURE 6 The steady-state coherence function calculated for the BChl866 antenna at room temperature for $N = 24$ (+) and $N = 32$ (○). Parameters were taken from fits 2 and 4 (see Table 1). The absolute values of $C(n)$ normalized to $C(0)$ are shown. The effective coherence length (FWHM) for both sets of parameters is $N_{coh} = 5.5$.

LH2 antenna of *R. acidophila* (Alden et al., 1997). It was shown that L remains below 0.1 over most of the B850 absorption band, indicating that the exciton wave functions are delocalized over more than 10 BChl850 molecules.

Notice that the inverse participation ratio corresponds to the delocalization length for the individual exciton states. However, in general we have always to deal with a superimposition of exciton states. For zero time delay (immediately after excitation), such a superimposition may exist because of the simultaneous excitation of several exciton levels by the short pulse. In the steady-state limit (for time delays longer than the exciton relaxation), we have to deal with a superimposition of states populated at thermal equilibrium. The evolution of the initially formed exciton wave packet into the steady-state wave packet can be described by the coherence function $C(n,t)$, defined as the off-diagonal element of the density matrix in the site representation, $\rho_{m,m+n}(t)$, averaged over the disorder and over m, where n and m are the molecular numbers (Meier et al., 1997; Kühn and Sundström, 1997). In the steady-state limit, the coherence function $C(n)$ is determined by the temperature-dependent populations of the exciton states (Meier et al., 1997). The delocalization length of the exciton wavepacket, N_{coh}, can be defined as an effective width (FWHM) of the coherence function. It can be shown that the N_{coh} value is approximately the same as the inverse participation ratio, N_{eff}, if only one exciton level is populated. But N_{coh} will be less than N_{eff} if we have to deal with an exciton wave packet.

The steady-state coherence functions for the BChl866 antenna for $N = 24$ and $N = 32$ are shown in Fig. 6. The M_{12} and σ values are from fits 2 and 4 (Table 1). We show the absolute values of $C(n)$ normalized to $C(0)$. The effective length of the exciton wave packet is the same for both cases, i.e., $N_{coh} = 5.5$. We have also calculated the steady-state coherence functions for $N = 24$ and different interaction energies (Fig. 7): the M_{12} and σ values are from fits 1–3 (Table 1). The coherence length of the exciton wave packet is $N_{coh} = 4.6$, 5.5, and 6.5, respectively. For comparison, Kühn and Sundström estimated the coherence length as four BChl molecules for the B850 antenna of *Rhodobacter sphaeroides*, taking $M_{12} = 300$ cm^{-1} and $\sigma = 700$ cm^{-1} (FWHM). In their model they have taken into account weak exciton-phonon coupling together with the static disorder (Kühn and Sundström, 1997).

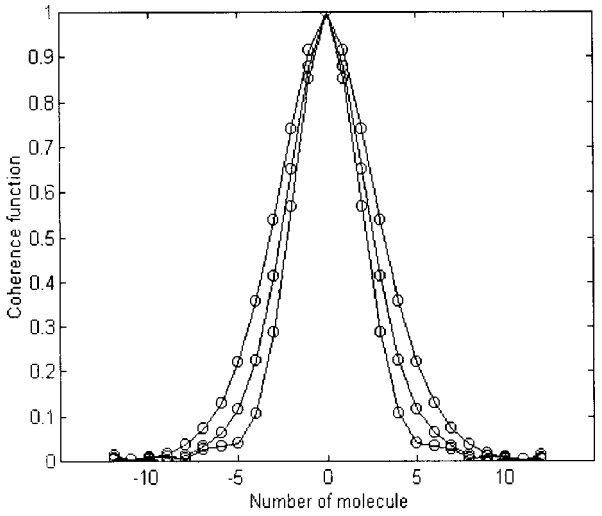

FIGURE 7 The steady-state coherence function calculated for the BChl866 antenna at room temperature for $N = 24$ and $M_{12} = 260$, 400, and 600 cm^{-1} (the lower interaction energy corresponds to the narrower coherence function). All other parameters were taken from fits 1–3 (see Table 1). The coherence length (FWHM) is $N_{coh} = 4.6$, 5.5, and 6.5, respectively.

CONCLUSION

We have proposed a model of the B808–866 BChl *a* antenna of the green photosynthetic bacterium *C. aurantiacus*. This antenna was assumed to be structurally similar to the LH2 antenna of purple bacteria, having the form of two concentric rings of N strongly coupled BChl866 pigments and of $N/2$ weakly coupled BChl808 monomers. The N value is most likely the same as for LH1 core antenna of purple bacteria, i.e., $N = 24$ or 32. The Q_y transition dipoles of BChl808 and BChl866 molecules form the angles $43° \pm 3°$ and $8° \pm 4°$, respectively, with the plane of the corresponding rings.

Using this model, we have obtained a quantitative fit of the pump-probe spectra of the B866 and B808 bands. From this fit we have estimated that the nearest-neighbor interaction energy in the BChl866 antenna is ~ 400 cm^{-1}, and the diagonal energy disorder is ~ 410 and ~ 600 cm^{-1} for $N = 24$ and 32, respectively. Using these values, we have demonstrated that the individual exciton states in the BChl866 antenna are highly delocalized (over 10–12 BChl molecules). The highly delocalized exciton wave functions of the BChl866 antenna are responsible for the anomalously high bleaching value of the B866 band with respect to that of the B808 monomeric band.

The population of several exciton levels in the steady-state limit gives rise to exciton wave packet formation. At room temperature its effective size is about five or six BChl866 molecules.

This work was supported by a grant from the Russian Foundation for Basic Research (99-04-49117 to ZGF).

REFERENCES

Agranovich, V. M., and M. D. Galanin. 1982. Electronic Excitation Energy Transfer in Condensed Matter. North-Holland, Amsterdam.

Alden, R. G., E. Johnson, V. Nagarajan, W. W. Parson, C. J. Law, and R. J. Cogdell. 1997. Calculation of spectroscopic properties of the LH2 bacteriochlorophyll-protein antenna compolex of *Rhodopseudomonas acidophila. J. Phys. Chem. B.* 101:4667–4680.

Chachisvilis, M., O. Kühn, T. Pullerits, and V. Sundström. 1997. Excitons in photosynthetic purple bacteria: wavelike motion or incoherent hopping? *J. Phys. Chem. B.* 101:7275–7283.

Davydov, A. S. 1971. Theory of Molecular Excitons. Plenum Press, New York.

Dracheva, T. V., V. I. Novoderezhkin, and A. P. Razjivin. 1995. Exciton theory of spectra and energy transfer in photosynthesis: spectral hole burning in the antenna of purple bacteria. *Chem. Phys.* 194:223–235.

Dracheva, T. V., V. I. Novoderezhkin, and A. P. Razjivin. 1996. Exciton delocalization in the antenna of purple bacteria: exciton spectra calculation using x-ray data and experimental site inhomogeneity. *FEBS Lett.* 378:81–84.

Dracheva, T. V., V. I. Novoderezhkin, and A. P. Razjivin. 1997. Exciton delocalization in the light-harvesting LH2 complex of photosynthetic purple bacteria. *Photochem. Photobiol.* 66(4):141–146.

Fidder, H., J. Knoester, and D. A. Wiersma. 1991. Optical properties of disordered molecular aggregates: a numerical study. *J. Chem. Phys.* 95:7880–7890.

Hu, X., T. Ritz, A. Damjanovic, and K. Shulten. 1997. Pigment organization and transfer of electronic excitation in the photosynthetic unit of purple bacteria. *J. Phys. Chem. B.* 101:3854–3871.

Jimenez, R., S. N. Dikshit, S. E. Bradforth, and G. R. Fleming. 1996. Electronic excitation transfer in the LH2 complex of *Rhodobacter sphaeroides. J. Phys. Chem.* 100:6825–6834.

Karrasch, S., P. A. Bullough, and R. Ghosh. 1995. The 8.5 A projection map of the light-harvesting complex I from *Rhodospirillum rubrum* reveals a ring composed of 16 subunits. *EMBO J.* 14–4:631–638.

Kennis, J. T. M., T. J. Aartsma, and J. Amesz. 1994. Energy trapping in the purple bacteria *Chromatium vinosum* and *Chromatium tepidum. Biochim. Biophys. Acta.* 1188:278–286.

Kennis, J. T. M., A. M. Streltsov, T. J. Aartsma, T. Nozava, and J. Amesz. 1996. Energy transfer and exciton coupling in isolated B800–850 complexes of the photosynthetic purple sulfur bacterium *Chromatium tepidum*. The effect of structural symmetry on bacteriochlorophyll excited states. *J. Phys. Chem.* 100:2438–2442.

Koepke, J., X. Hu, C. Muenke, K. Schulten, and H. Michel. 1996. The crystal structure of the light-harvesting complex II (B800–850) from *Rhodospirillum molischianum. Structure.* 4:581–597.

Koolhaas, M. H. C., G. van der Zwan, R. N. Frese, and R. van Grondelle. 1997. Red shift of the zero crossing in the CD spectra of the LH2 antenna complex of *Rhodopseudomonas acidophila:* a structure-based study. *J. Phys. Chem. B.* 101:7262–7270.

Kühn, O., and V. Sundström. 1997. Pump-probe spectroscopy of dissipative energy transfer dynamics in photosynthetic antenna complexes: a density matrix approach. *J. Chem. Phys.* 107:4154–4164.

Leupold, D., H. Stiel, K. Teuchner, F. Novak, W. Sandner, B. Ucker, and H. Scheer. 1996. Size enhancement of transition dipoles to one- and two-exciton bands in a photosynthetic antenna. *Phys. Rev. Lett.* 77: 4675–4678.

McDermott, G., S. M. Prince, A. A. Freer, A. M. Hawthornthwaite-Lawless, M. Z. Papiz, R. J. Cogdell, and N. W. Isaacs. 1995. Crystal structure of an integral membrane light-harvesting complex from photosynthetic bacteria. *Nature.* 374:517–521.

Meier, T., V. Chernyak, and S. Mukamel. 1997. Multiple exciton coherence sizes in photosynthetic antenna complexes viewed by pump-probe spectroscopy. *J. Phys. Chem. B.* 101:7332–7342.

Monshouwer, R., M. Abrahamsson, F. van Mourik, and R. van Grondelle. 1997. Superradiance and exciton delocalization in bacterial photosynthetic light-harvesting systems. *J. Phys. Chem. B.* 101:7241–7248.

Mukamel, S. 1995. Principles of Nonlinear Optical Spectroscopy. Oxford University Press, New York, Oxford.

Novoderezhkin, V. I., and A. P. Razjivin. 1993. Excitonic interactions in the light-harvesting antenna of photosynthetic purple bacteria and their influence on picosecond absorbance difference spectra. *FEBS Lett.* 330: 5–7.

Novoderezhkin, V. I., and A. P. Razjivin. 1994. Exciton states of the antenna and energy trapping by the reaction center. *Photosynth. Res.* 42:9–15.

Novoderezhkin, V. I., and A. P. Razjivin. 1995a. Exciton dynamics in circular aggregates: application to antenna of photosynthetic purple bacteria. *Biophys. J.* 68:1089–1100.

Novoderezhkin, V. I., and A. P. Razjivin. 1995b. Excitation delocalizaiton over the whole core antenna of photosynthetic purple bacteria evidenced by non-linear pump-probe spectroscopy. *FEBS Lett.* 368:370–372.

Novoderezhkin, V. I., A. S. Taisova, Z. G. Fetrisova, R. E. Blankenship, S. Savikhin, D. R. Buck, and W. S. Struve. 1998. Energy transfers in the B808–866 antenna from the green bacterium *Chloroflexus aurantiacus. Biophys. J.* 74:2069–2075.

Pullerits, T., M. Chachisvilis, and V. Sundström. 1996. Exciton delocalization length in the B850 antenna of *Rhodobacter sphaeroides. J. Phys. Chem.* 100:10787–10792.

Pullerits, T., K. J. Visscher, S. Hess, V. Sundström, A. Freiberg, K. Timpmann, and R. van Grondelle. 1994. Energy transfer in the inhomogeneously broadened core antenna of purple bacteria: a simultaneous fit of low-intensity picosecond absorption and fluorescence kinetics. *Biophys. J.* 66:236–248.

Somsen, O. J. G., F. van Mourik, R. van Grondelle, and L. Valkunas. 1994. Energy migration and trapping in a spectrally and spatially inhomogeneous light-harvesting antenna. *Biophys. J.* 66:1580–1596.

van Burgel, M., D. A. Wiersma, and K. Duppen. 1995. The dynamics of one-dimensional excitons in liquids. *J. Chem. Phys.* 102:20–33.

van Grondelle, R., J. P. Dekker, T. Gillbro, and V. Sundström. 1994. Energy transfer and trapping in photosynthesis. *Biochim. Biophys. Acta.* 1187:1–65.

Vasmel, H., R. J. van Dorssen, G. J. de Vos, and J. Amesz. 1986. Pigment organization and energy transfer in the green photosynthetic bacterium *Chloroflexus aurantiacus*. I. The cytoplasmic membrane. *Photosynth. Res.* 7:281–294.

Visser, H. M., O. J. G. Somsen, F. van Mourik, S. Lin, I. H. M. van Stokkum, and R. van Grondelle. 1995. Direct observation of sub-picosecond equilibration of excitation energy in the light-harvesting antenna of *Rhodospirillum rubrum. Biophys. J.* 69:1083–1099.

Wechsler, T. D., R. A. Brunisholz, G. Frank, F. Suter, and H. Zuber. 1987. The complete amino acid sequence of the antenna polypeptide B806–866-β from the cytoplasmic membrane of the green bacterium *Chloroflexus aurantiacus. FEBS Lett.* 210:189–194.

Wechsler, T., R. Brunisholz, F. Suter, R. C. Fuller, and H. Zuber. 1985. The complete amino acid sequence of a bacteriochlorophyll *a* binding polypeptide isolated from the cytoplasmic membrane of the green photosynthetic bacterium *Chloroflexus aurantiacus. FEBS Lett.* 191:34–38.

Xiao, W., S. Lin, A. K. W. Taguchi, and N. W. Woodbury. 1994. Femtosecond pump-probe analysis of energy and electron transfer in photosynthetic membranes of *Rhodobacter capsulatus. Biochemistry.* 33: 8313–8322.

Zuber, H., and R. A. Brunisholz. 1991. Structure and function of antenna polypeptides and chlorophyll-protein complexes: principles and variability. *In* Chlorophylls. H. Scheer, editor. CRC Press, Boca Raton, FL. 628–692.